Tracking Control of Underwater Vehicles Based on Adaptive Nonlinear Robust Inner/Outer Loop Approach

Fahimeh S. Tabatabaee-Nasab[1,2], S. Ali Akbar Moosavian[1,2]*

1- Center of Excellence in Robotics and Control, Advanced Robotics & Automated Systems (ARAS) Laboratory

2- Department of Mechanical Engineering, K. N. Toosi University of Technology, Tehran, Iran

* Email: tabatabaenasab@gmail.com, Moosavian@kntu.ac.ir

Highly nonlinear systems with parametric uncertainties and external disturbances deteriorate the tracking control performance of autonomous underwater vehicles. In this research, to attain an optimal precision, an adaptive integral-type terminal sliding mode controller is proposed. To this end, the kinematics and kinetics controller laws are developed as the outer and inner loop control to track desired trajectories. The kinematics controller, as the outer controller, is developed to control the position errors. The kinetics controller, as the inner servo loop, is developed based on the system dynamics model and an adaptive integral-exponential sliding surface to control the internal velocity errors. In order to enhance the control proficiency, we have implemented an adaptive switching rule within the kinetic control algorithm, enabling an automated adjustment of all controller parameters. Therefore, the increase and decrease of these switching parameters will occur according to the system conditions, while its stability is guaranteed using Lyapunov theorems. Obtained results show the merits of the proposed controller in terms of high accuracy performance and low computation cost for real-time implementations.

Keywords — Adaptive Terminal Sliding Mode Control, Position Control, Autonomous Underwater Vehicles (AUV), Trajectory tracking.

1. Introduction

In recent years, sophisticated submersible robots have become integral to underwater research and exploration efforts. These robots are utilized in various commercial, military, and scientific endeavors, as well as mapping initiatives, effectively reducing the need for human intervention. The exceptional capabilities of automated underwater robots, particularly in executing complex oceanic missions at significant depths, have solidified their pivotal role in the industry [1]. The primary focus of research on mobile robots in this category revolves around the complex challenges associated with modeling these systems. These challenges include nonlinear equations, uncertainties in both structural and non-structural aspects, environmental dependencies on model parameters, and external disturbances such as ocean currents. The intricate nature of these factors makes the study of these systems particularly enticing yet intricate [2]. Hence, extensive research has been dedicated to the dynamic analysis and design of control algorithms for these systems. Numerous studies have focused on the fields of system identification, modeling, and control methods in order to enhance the autonomy of these devices. Given the challenging operational environments in which these devices are deployed, it is essential to develop control techniques that not only offer high accuracy but also demonstrate robustness against external disturbances and noise attenuation capabilities [3]. To address these requirements, a variety of control methods have been suggested, including sliding mode controller [4-7], high-order sliding mode controller [8], backstepping sliding mode controller [9], adaptive controller [10-11], optimal controller [12-13], and fuzzy controller [14].

In sliding mode, the nonlinear closed-loop control system is insensitive to uncertain dynamics and averts bounded input disturbances. However, in the worst-case scenario, knowing uncertainty bounds is essential when planning of the sliding mode and robust controllers [15,16]. Therefore,

controller design can be extremely conservative that can decline the velocity of the closed-loop response. Considering the above characteristics, sliding mode control along with adaptive mechanisms is suitable for nonlinear and fast response applications.

Fussen [17] introduced an adaptive sliding mode controller for submarine robots which compensates for the uncertainty of the input matrix by adding a discrete term (sliding mode term) to an adaptive controller. This uncertainty is created due to the time-variant behavior of control input caused by feeder hydraulics. In [18] proposed an adaptive sliding mode control method for controlling an AUV in the vertical sheet which employs stare error as the feedback signal to update the linear parameter for compensating for linear uncertainties. Yoerger [19] empirically developed an adaptive sliding mode control for an AUV in which a nonlinear system model was used. When extended disturbances of system state exceed the tolerance layer of the sliding mode, this excess value is used to update the nonlinear model parameters and control inputs. Thus, this controller compensates for changes in the environment. Corradini [20] proposed an adaptive sliding mode controller which adjusts the sliding mode parameters based on the estimation of system parameter bounds. [21, 22] demonstrate the adaptive sliding mode tracking controller for entirely operated AUVs. Maghooli et al. [23] suggested a self-tuning robust tracking control that is independent, and contains known/unknown parts to control the AUV.

Motivated by the above a new optimal self-tunning tracking control based on robust inner-loop system is presented in this paper to solve the trajectory tracking problem of the AUV subjected to uncurtains and external disturbances. By employing nonlinear adaptive sliding surfaces, the sliding manifolds can rapidly converge. The AUV system incorporates adaptive sliding mode surfaces that utilize fractional derivative and integral to enhance the speed of the attitude states. To this end, the kinematic and kinetic controller laws are designed as the outer and inner loop control to track

desired trajectories. The kinematics controller, as the outer controller, is developed to optimal self-tuning control. The kinetics controller, as the inner servo loop, is developed based on adaptive nonsingular fast terminal sliding mode control law is further developed, and enhances the robustness of the AUV in the presence of external disturbances and uncertainties. Furthermore, the fluctuation in switching parameters occurs in accordance with the system's conditions, with the assurance of stability achieved through the application of Lyapunov theories.

The current research effort showcases significant contributions as listed below:

(i) The AUV has been fortified with a meticulously devised optimal self-tuning control mechanism employing the sequential quadratic programming algorithm. Such an approach emanates substantial advantages for the AUV control system, notably in terms of expeditious trajectory tracking performance and rapid finite-time convergence.

(ii) Adaptive laws, which are predicated solely on velocity and position information, have been introduced to effectively contend with the upper bound of uncertainties and disturbances. These adaptive laws manifest realism and practicability.

(iii) After conducting a thorough comparative analysis of alternative controllers, it can be confidently affirmed that the proposed controller has been found to be highly effective and its efficacy has been comprehensively ascertained.

The remainder of this document is structured in the following manner: section 2 describes the kinematics and kinetics modeling of the AUV with/without uncertainties. In Section 3, an analytical description of the proposed algorithm and stability analysis are presented. Section 4 is illustrated obtained results compared with other methods, and finally, section 5, concludes this work.

2. Preliminaries and Mathematical Modeling

2.1. North-East-Down (n-frame): NED

This system is usually defined as a plane tangential to the ground surface that moves with the vessel's motion. Still, the direction of its axes is different from the direction of the axes of the body coordinate system (which is described below). For this system, the x-axis is northing, the y-axis is easting, and the z-axis is perpendicular to the ground surface and toward its center. The position of the NED coordinate system relative to the ECE coordinate system is determined by latitude and longitude.

This coordinate system is used to navigate vessels operating in a restricted area. For these vessels, this coordinate system can be considered a bare coordinate system governed by Newton's laws.

2.2. Body Frame

The body coordinate system is a moving coordinate device fixed on a vessel. The position of marine vessels is described relative to a bare device, while the linear velocities and angles of a vessel are defined in the body coordinate system. In submarine boat, the origin of the body coordinate system is usually located in the center of mass or the center of buoyancy, and its axes are considered in the direction of the vessel's motion, as shown in Fig. 1.

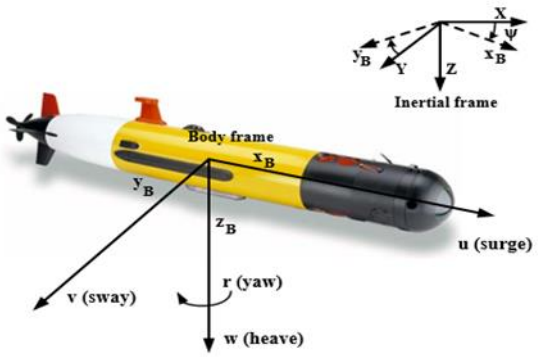

Fig1. Underwater vehicle (REMUS 100)

The pose vector of the AUV concerning the fixed frame is denoted by $\eta = [\eta_1 \ \eta_2]^T \in \mathcal{R}^6$. (i.e., $\eta_1 = [x \ y \ z]^T$: the position vectors and i.e., $\eta_2 = [\phi \ \theta \ \psi]^T$: the orientation vectors.

The $v = [v_1 \ v_2]^T \in \mathcal{R}^6$ is the velocity vector of the AUV expressed in body frame. (i.e., $v_1 = [u \ v \ w]^T$: the linear velocity vectors, and i.e., $v_2 = [p \ q \ r]^T$: the angular velocity vectors)

2.3. Mathematical Modeling

The kinematic and kinetics equations of the AUV [10] can be successfully acquired by employing the esteemed Eq. (1).

$$\dot{\eta} = j(\eta)\upsilon \qquad (1a)$$

$$\tau = M\dot{\upsilon} + C(\upsilon)\upsilon + D(\upsilon)\upsilon + g(\eta) \qquad (1b)$$

Where

- $\tau = [X, Y, Z, K, M, N]^T \in \mathcal{R}^6$ symbolizes the comprehensive applied propulsion force or torque vector on the AUV;
- $M = M_{RB} + M_A$ where $M_{RB} \in \mathcal{R}^{6\times6}$ and $M_A \in \mathcal{R}^{6\times6}$ represent the inertia matrix for the rigid body, and additionally includes the added mass contribution.;
- $C(v) = C_{RB}(v) + C_A(v)$ where $C_{RB}(v) \in \mathcal{R}^{6\times6}$ and $C_A(v) \in \mathcal{R}^{6\times6}$ represents the Coriolis and centripetal matrix, respectively;
- $D(v) = D_{RB}(v) + D_A(v)$ where $D_{RB}(v) \in \mathcal{R}^{6\times6}$ and $D_A(v) \in \mathcal{R}^{6\times6}$ represent the combined effect of quadratic and linear drag.;
- $g(\eta) \in \mathcal{R}^{6\times6}$ constitutes the vector that represents the hydrostatic restoring force;
- $j(\eta) = \begin{bmatrix} j_1(\eta_2) & 0_{3\times3} \\ 0_{3\times3} & j_2(\eta_2) \end{bmatrix}$ is the Jacobian matrix;

The properties of this model include the following:

The added mass matrix M is a definite positive matrix with constant values

$$M = M^T > 0$$

For a rigid body moving in a fluid, the Coriolis and centrifugal matrix $C(v)$ is a Skew-symmetric matrix so that.

$$C(v) = -C(v)^T > 0, \forall v \in R^6$$

For a rigid body moving in a fluid, the hydrodynamic damping matrix is a definite real, asymmetric, and positive matrix so that.

$$D(v) > 0, \forall v \in R^6$$

3. Mathematical Modeling in the Presence of Uncertainties

Generally, there are inaccuracies and uncertainties in modeling a dynamic model such as an AUV. Uncertainties in dynamic model parameters are unavoidable, taking into account the complexies of modeling the equipment movement within a fluid environment.

Due to the uncertainties and dynamic modeling errors, the actual values of the parameters $\mathcal{M}$, $\mathcal{C}(\vartheta)$, and $\mathcal{D}(\vartheta)$ in Eq. (1) are the sum of the approximately known parts ($\mathcal{M}^{\dagger}$, $\mathcal{C}^{\dagger}(\vartheta)$, and $\mathcal{D}^{\dagger}(\vartheta)$), and unknown parts of the parameters ($\Delta\mathcal{M}$, $\Delta\mathcal{C}(\vartheta)$, and $\Delta\mathcal{D}(\vartheta)$).

Thus, the model of the AUV with known/unknown parts can be aptly articulated as follows:

$$\tau = \mathcal{M}^{\dagger}\dot{\vartheta} + \mathcal{C}^{\dagger}(\vartheta)\vartheta + \mathcal{D}^{\dagger}(\vartheta)\vartheta + \Delta\mathcal{M}\dot{\vartheta} + \Delta\mathcal{C}(\vartheta)\vartheta + \Delta\mathcal{D}(\vartheta)\vartheta + d \tag{2}$$

Where d represent the external disturbances.

Thus, model uncertainties can be defined in the following forms:

$$\delta_{\vartheta} = \Delta\mathcal{M}\dot{\vartheta} + \Delta\mathcal{C}(\vartheta)\vartheta + \Delta\mathcal{D}(\vartheta)\vartheta + d \tag{3}$$

Substituting (3) into (2), one acquires:

$$\tau = \mathcal{M}^{\dagger}\dot{\vartheta} + \mathcal{C}^{\dagger}(\vartheta)\vartheta + \mathcal{D}^{\dagger}(\vartheta)\vartheta + \delta_{\vartheta} \tag{4}$$

Thus, $\dot{\vartheta}$ can be computed utilizing the following expression:

$$\dot{\vartheta} = \mathcal{M}^{\dagger-1}\left(\tau - \mathcal{C}^{\dagger}(\vartheta)\vartheta - \mathcal{D}^{\dagger}(\vartheta)\vartheta - \delta_{\vartheta}\right) \tag{5}$$

Calculating (6) by substituting (5) into (4):

$$\delta_{\vartheta} = \Delta\mathcal{M}\mathcal{M}^{\dagger-1}\left(\tau - \mathcal{C}^{\dagger}(\vartheta)\vartheta - \mathcal{D}^{\dagger}(\vartheta)\vartheta - \delta\right) + \Delta\mathcal{C}(\vartheta)\vartheta + \Delta\mathcal{D}(\vartheta)\vartheta + d \tag{6}$$

Simplifications yield:

$$\delta_{\vartheta} = \left(\mathrm{I} + \Delta\mathcal{M}\mathcal{M}^{\dagger-1}\right)^{-1}\left\{\Delta\mathcal{M}\mathcal{M}^{\dagger-1}\left(\tau - \mathcal{C}^{\dagger}\left(\vartheta\right)\vartheta - \mathcal{D}^{\dagger}\left(\vartheta\right)\vartheta\right) + \Delta\mathcal{C}\left(\vartheta\right)\vartheta + \Delta\mathcal{D}\left(\vartheta\right)\vartheta + d\right\} \tag{7}$$

Therefore, δ (external disturbances and system uncertainties) is upper bounded as

$$\begin{aligned}\delta_{\vartheta} \leq\\ \left(\mathrm{I} + \Delta\mathcal{M}\mathcal{M}^{\dagger-1}\right)^{-1}\Delta\mathcal{M}\mathcal{M}^{\dagger-1} \times \left\{\tau + \mathcal{C}^{\dagger}\left(\vartheta\right)\vartheta + \mathcal{D}^{\dagger}\left(\vartheta\right)\vartheta\right\} +\\ \left(\mathrm{I} + \Delta\mathcal{M}\mathcal{M}^{\dagger-1}\right)^{-1}\left\{\Delta\mathcal{C}\left(\vartheta\right)\vartheta + \Delta\mathcal{D}\left(\vartheta\right)\vartheta + d\right\}\end{aligned} \tag{8}$$

Equivalent to the essence of mechanical systems, it is assumed that [10]:

1) The norm of inertia mass is upper bounded as

$$\mathcal{M} < \alpha_0 \tag{9}$$

2) The norm of the Coriolis matrix and centripetal terms ($\mathcal{C}(\vartheta) \in \Re^{4\times4}$) are upper bounded as

$$\mathcal{C}\left(\vartheta\right) < \alpha_1\vartheta + \alpha_2 \tag{10}$$

3) The norm of the damping matrix ($\mathcal{D}(\vartheta) \in \Re^{4\times4}$) is upper bounded as

$$\mathcal{D}\left(\vartheta\right) < \alpha_3\vartheta + \alpha_4 \tag{11}$$

Based on the dynamic model of AUV, the upper bound for the magnitude of the actuator forces vector is constrained to follow the norm.

(12)

Thus, the norm of δ is upper bounded as

$$\tau < \alpha_5\vartheta + \alpha_6 \;\; \delta_{\vartheta} \leq \gamma_0 + \gamma_1\vartheta + \gamma_2\vartheta^2 \tag{13}$$

in which α_i $(i = \{0, .., 6\})$ & γ_i $(i = \{0, ..., 2\})$ are precisely set as the upper bounds for the dynamic model uncertainties.

4. Methodology

Fig. 2 displays the intended control framework for AUV.

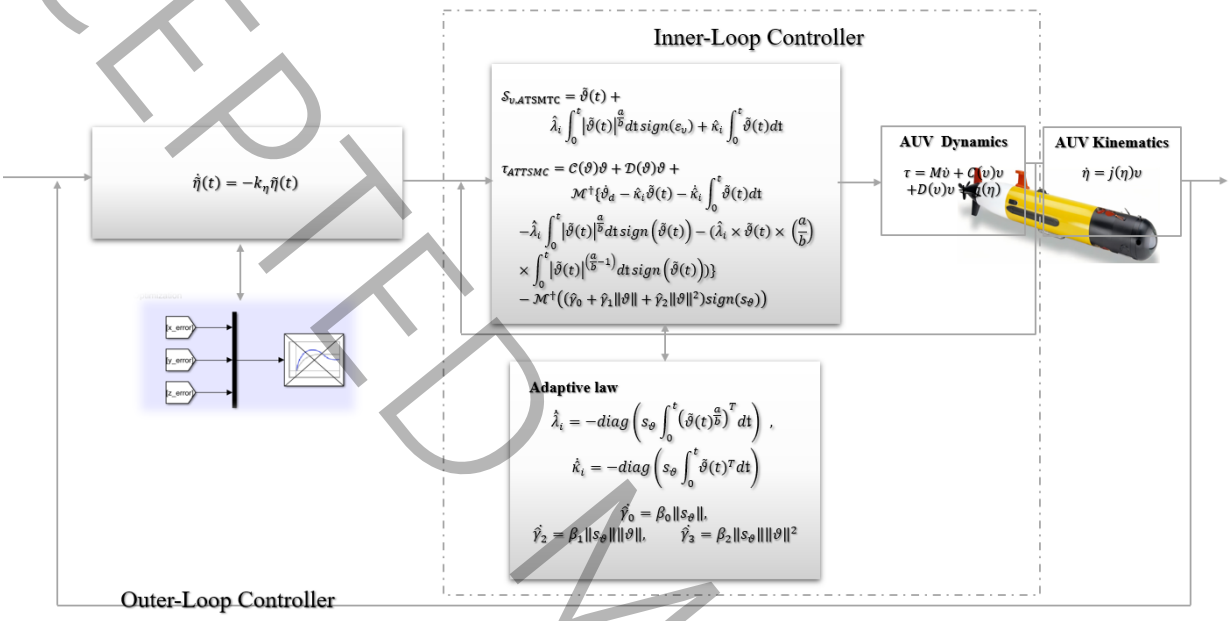

Fig. 2. The proposed control algorithm for trajectory tracking

3.1 Geometry of Workspace

The reference trajectory for the AUV in Cartesian space is expressed as time-dependent functions.

$$\eta_d = \eta_d(t) \tag{14}$$

Utilizing the envisioned path and the recorded output signal, the tracking errors can be precisely characterized as:

$$\tilde{\eta}(t) = \eta(t) - \eta_d(t) \tag{15}$$

3.2 Outer-Loop Controller

A. Optimal Self-Tunning Controller

As a fundamental principle, the control law known as Proportional-Integral-Derivative can be expressed in the following manner:

$$\vartheta_c = K_P\left[\varepsilon_\eta(t)\right] + K_I\left[\int \varepsilon_\eta(t)dt\right] + K_D\left[\frac{d}{dt}\varepsilon_\eta(t)\right] \tag{16}$$

The arduous aspect of this design lies in the determination of the optimal values for these nine constant parameters, which would bring about the most favorable response from the system. In this paper, the parameters of the control law (K_{P_i}, K_{I_i}, K_{D_i}) have been estimated using the Sequential Quadratic Programming algorithm.

3.3 Inner Loop controller

5. *Feedback linearizing control (FLC)*

The initial regulator of the dynamic portion is depicted utilizing the FLC. Thus, tracking error is determined as:

$$\mathcal{E}_\vartheta = \vartheta_c - \vartheta \tag{17}$$

Where ϑ_c represents a kinematic input vector achieved from the kinematic controller design. Thus, the control law is:

$$\tau = \mathcal{M}\dot{\vartheta}_c + \mathcal{C}(\vartheta)\vartheta + \mathcal{D}(\vartheta)\vartheta + \mathcal{M}\mathcal{K}\mathcal{E}_\vartheta \tag{18}$$

Where $\mathcal{K}$ shows the gain matrix of the system.

Proposition 2: Tracking error of system velocities is stabilized by the control law of Eq. (18) for dynamic systems about origin asymptotically (Eq.1).

Proof: To guarantee the closed-loop system's stability, the candidate Lyapunov function is chosen as in Eq. (19).

$$V_{\text{FLDC}} = \frac{1}{2}\mathcal{E}_{\vartheta}^{T}\mathcal{E}_{\vartheta} \tag{19}$$

The chosen Lyapunov function's time derivative is explained in Eq. (20).

$$\dot{V}_{\text{FLDC}} = \mathcal{E}_{\vartheta}^{T}\dot{\mathcal{E}}_{\vartheta} = \mathcal{E}_{\vartheta}^{\text{T}}\left(\dot{\vartheta}_{c} - \dot{\vartheta}\right) \tag{20}$$

To obtain Eq. (21) dynamic model of Eq. (1) are replaced, and control inputs of Eq. (18) are applied.

$$\dot{V}_{\text{NDC}} = \mathcal{E}_{\vartheta}^{T}\left(\mathcal{M}^{-1}\left\{\tau - \mathcal{C}\left(\vartheta\right)\vartheta - \mathcal{D}\left(\vartheta\right)\vartheta - \mathcal{M}\mathcal{K}\mathcal{E}_{\vartheta}\right\} - \mathcal{M}^{-1}\left\{\tau - \mathcal{C}\left(\vartheta\right)\vartheta - \mathcal{D}\left(\vartheta\right)\vartheta\right\}\right) \tag{21}$$

Simplifications yield

$$\dot{V}_{NDC} = -\mathcal{E}_{\vartheta}^{T}\mathcal{K}\mathcal{E}_{\vartheta} \tag{22}$$

Hence, the derivative of the positive definite Lyapunov function needs to be negative to realize the convergence of the velocity errors and system stability. Thus, coefficients $\mathcal{K}$ must be positive.

6. Sliding mode control (SMC)

Sliding mode control possesses features such as robustness against parametric and structural uncertainties. Moreover, it has the proper transient response, which discriminates it from other control approaches.

PI filtered tracking error as the sliding surface is determined (Eq.23), where $\mathcal{K}$ shows the gain matrix of the sliding surface integrator.

$$S_{\vartheta} = \mathcal{E}_{\vartheta} + \mathcal{K}\int_{0}^{t}\mathcal{E}_{\vartheta}\left(\tau\right)d\tau \tag{23}$$

Take SMDC control law into account, as in Eq. (24).

$$\tau = \mathcal{M}\dot{\vartheta}_c + \mathcal{C}(\vartheta)\vartheta + \mathcal{D}(\vartheta)\vartheta + \mathcal{M}\mathcal{K}\mathcal{E}_\vartheta - \mathcal{K}_s S_\vartheta - W_s \operatorname{sgn}(S_\vartheta) \tag{24}$$

Where $\mathcal{K}_s$, and W_s are the control gains of the system.

Proposition 3: For the AUV, the tracking error of the system velocities is stabilized by the control law of Eq. (24) about the origin asymptotically (Eq.1).

Proof: The definitely positive function of Eq. (25) is considered a Lyapunov function.

$$V_{\text{SMDC}} = \frac{1}{2} S_\vartheta^T S_\vartheta \tag{25}$$

This function's time derivative is expressed in Eq. (26).

$$\dot{V}_{\text{SMDC}} = S_\vartheta^T \dot{S}_\vartheta = S_\vartheta^{\mathrm{T}} \left(\dot{\mathcal{E}}_\vartheta + \mathcal{K}\mathcal{E}_\vartheta\right) \tag{26}$$

Eq. (26) can be simplified as in Eq. (27) through the control input of Eq. (24) and the dynamic model.

$$\dot{V}_{\text{SMDC}} = S_\vartheta^{\mathrm{T}} \left(-\mathcal{K}_s S_\vartheta - W_s \operatorname{sgn}(S_\vartheta)\right) \tag{27}$$

Hence, in order to attain system stability, it is imperative that the derivative of the positive definite Lyapunov function demonstrates negativity. Therefore, coefficients $\mathcal{K}_s$, and W_s must be positive.

7. Adaptive fast Terminal sliding mode dynamic controller

AUVs find significant utilization in various challenging and diverse habitats, primarily exemplified by expansive and unpredictable oceanic settings. Consequently, it becomes imperative to devise control approaches that not only exhibit exceptional precision but also exhibit unwavering resilience to disruptive external factors. Sliding-mode controller is one of the control methods which have these characteristics. To this end, the integral-exponential sliding surface is defined based on velocity tracking error as in Eq. (28).

$$\mathcal{S}_{\upsilon,\mathrm{TSMTC}} = \tilde{\vartheta}(t) + \lambda \int_0^t \left|\tilde{\vartheta}(t)\right|^{\frac{a}{b}} d\,\mathrm{t}\, sign\left(\varepsilon_\upsilon\right) + \kappa \int_0^t \tilde{\vartheta}(t) d\,\mathrm{t} \tag{28}$$

Where λ and κ are positive constants, a, and b are positive odd integers satisfying $0 < \frac{a}{b} < 1$.

The FTSMC scheme eliminates the offset, and the steady state errors converge to zero.

The adaptive integral-exponential sliding surface is defined based on velocity tracking error as in Eq. (29).

$$\mathcal{S}_{\upsilon,\mathrm{TSMTC}} = \tilde{\vartheta}(t) + \hat{\lambda}_i \int_0^t \left|\tilde{\vartheta}(t)\right|^{\frac{a}{b}} d\,\mathrm{t}\, sign\left(\varepsilon_\upsilon\right) + \hat{\kappa}_i \int_0^t \tilde{\vartheta}(t) d\,\mathrm{t} \tag{29}$$

The following ATSMC law:

$$\begin{aligned} \tau_{\mathrm{ATTSMC}} = {} & \mathcal{C}(\vartheta)\dot{\vartheta} + \mathcal{D}(\vartheta)\vartheta + \mathcal{M}^{\dagger}\{\dot{\vartheta}_d - \dot{\hat{\kappa}}_i \tilde{\vartheta}(t) - \dot{\hat{\kappa}}_i \int_0^t \tilde{\vartheta}(t) d\,\mathrm{t} \\ & - \dot{\hat{\lambda}}_i \int_0^t \left|\tilde{\vartheta}(t)\right|^{\frac{a}{b}} d\,\mathrm{t}\, sign\left(\tilde{\vartheta}(t)\right) - \left(\hat{\lambda}_i \times \tilde{\vartheta}(t) \times \left(\frac{a}{b}\right) \times \int_0^t \left|\tilde{\vartheta}(t)\right|^{\left(\frac{a}{b}-1\right)} d\,\mathrm{t}\, sign\left(\tilde{\vartheta}(t)\right)\right)\} \\ & - \mathcal{M}^{\dagger}\left(\left(\hat{\gamma}_0 + \hat{\gamma}_1\vartheta + \hat{\gamma}_2\vartheta^2\right)\mathrm{sign}\left(s_\vartheta\right)\right) \end{aligned} \tag{30}$$

The following adaptive rules are used to obtain the control parameters of the sliding surfaces and the switching control law:

$$\dot{\hat{\lambda}}_i = -\mathrm{diag}\left(s_\vartheta \int_0^t \left(\tilde{\vartheta}(t)^{\frac{a}{b}}\right)^T d\,\mathrm{t}\right),\ \dot{\hat{\kappa}}_i = -\mathrm{diag}\left(s_\vartheta \int_0^t \tilde{\vartheta}(t)^T d\,\mathrm{t}\right) \tag{31}$$

$$\dot{\hat{\gamma}}_0 = \beta_0 s_\vartheta, \dot{\hat{\gamma}}_2 = \beta_1 s_\vartheta \vartheta, \dot{\hat{\gamma}}_3 = \beta_2 s_\vartheta \vartheta^2$$

The estimation error in calculating these parameters can be described as follows.

$$\tilde{\gamma} = \hat{\gamma} - \gamma_0 \tag{32}$$

Proof: Considering the following Lyapunov function candidate:

$$V_{\text{APISMC}}\left(s_{\vartheta},\tilde{\mathcal{Q}}\right)=\frac{1}{2}\tilde{\mathcal{Q}}^{\mathrm{T}}\mathrm{L}\tilde{\mathcal{Q}}+\frac{1}{2}\sum s_{\vartheta}^{2} \tag{33}$$

Where:

$$\tilde{\mathcal{Q}}=\left[\tilde{\gamma}_i\right]^T,\mathrm{L}=\mathrm{diag}\left[\beta_0{}^{-1},\beta_1{}^{-1},\beta_2{}^{-1}\right]^T \tag{34}$$

The function candidate time derivative is obtained as:

$$\dot{V}_{\text{APISMC}}\left(s_{\vartheta},\tilde{\mathcal{Q}}\right)=\tilde{\mathcal{Q}}^{\mathrm{T}}\mathrm{L}\dot{\tilde{\mathcal{Q}}}+\sum s_{\vartheta}^{T}\dot{s}_{\vartheta}=\tilde{\mathcal{Q}}^{\mathrm{T}}\mathrm{L}\dot{\tilde{\mathcal{Q}}}+\sum s_{\vartheta}^{T}\{\dot{\vartheta}_d-\dot{\vartheta}-\dot{\hat{\kappa}}_i\tilde{\vartheta}(t)-\hat{\kappa}_i\tilde{\vartheta}(t)-\dot{\hat{\kappa}}_i\int_0^t\tilde{\vartheta}(t)dt \tag{35}$$

$$-\dot{\hat{\lambda}}_i\int_0^t\left|\tilde{\vartheta}(t)\right|^{\frac{a}{b}}dt\,\mathrm{sign}\left(\tilde{\vartheta}(t)\right)-\left(\hat{\lambda}_i*\tilde{\vartheta}(t)\times\left(\frac{a}{b}\right)\times\int_0^t\left|\tilde{\vartheta}(t)\right|^{\left(\frac{a}{b}-1\right)}dt\,\mathrm{sign}\left(\tilde{\vartheta}(t)\right)\right)\}$$

$$=\tilde{\mathcal{Q}}^{\mathrm{T}}\mathrm{L}\dot{\tilde{\mathcal{Q}}}+\sum s_{\vartheta}^{T}\{\dot{\vartheta}_d-\mathcal{M}^{\dagger-1}\left(\tau-\mathcal{C}^{\dagger}\left(\vartheta\right)\vartheta-\mathcal{D}^{\dagger}\left(\vartheta\right)\vartheta-\delta_{\vartheta}\right)-\dot{\hat{\kappa}}_i\tilde{\vartheta}(t)-\hat{\kappa}_i\tilde{\vartheta}(t)-\dot{\hat{\kappa}}_i\int_0^t\tilde{\vartheta}(t)dt$$

$$-\dot{\hat{\lambda}}_i\int_0^t\left|\tilde{\vartheta}(t)\right|^{\frac{a}{b}}dt\,\mathrm{sign}\left(\tilde{\vartheta}(t)\right)-\left(\hat{\lambda}_i\times\tilde{\vartheta}(t)\times\left(\frac{a}{b}\right)\times\int_0^t\left|\tilde{\vartheta}(t)\right|^{\left(\frac{a}{b}-1\right)}dt\,\mathrm{sign}\left(\tilde{\vartheta}(t)\right)\right)\}$$

$$=\tilde{\mathcal{Q}}^{\mathrm{T}}\mathrm{L}\dot{\tilde{\mathcal{Q}}}+\sum s_{\vartheta}^{T}\{\dot{\vartheta}_d$$

$$-\mathcal{M}^{\dagger-1}$$

$$\left(\mathcal{C}(\vartheta)\vartheta+\mathcal{D}(\vartheta)\vartheta+\mathcal{M}^{\dagger}\{\dot{\vartheta}_d-\dot{\hat{\kappa}}_i\tilde{\vartheta}(t)-\hat{\kappa}_i\int_0^t\tilde{\vartheta}(t)dt-\dot{\hat{\lambda}}_i\int_0^t\left|\tilde{\vartheta}(t)\right|^{\frac{a}{b}}dt\,\mathrm{sign}\left(\tilde{\vartheta}(t)\right)-\left(\hat{\lambda}_i\times\tilde{\vartheta}(t)\times\left(\frac{a}{b}\right)\times\int_0^t\left|\tilde{\vartheta}(t)\right|^{\left(\frac{a}{b}-\right.}\right.\right.\right.$$

$$\left.\left.\left.-\mathcal{C}^{\dagger}(\vartheta)\vartheta-\mathcal{D}^{\dagger}(\vartheta)\vartheta-\delta_{\vartheta}\right)\right.\right.$$

$$-\dot{\hat{\kappa}}_i\tilde{\vartheta}(t)-\hat{\kappa}_i\int_0^t\tilde{\vartheta}(t)dt$$

$$-\dot{\hat{\lambda}}_i\int_0^t\left|\tilde{\vartheta}(t)\right|^{\frac{a}{b}}dt\,\mathrm{sign}\left(\tilde{\vartheta}(t)\right)-$$

$$\left(\hat{\lambda}_i\times\tilde{\vartheta}(t)\times\left(\frac{a}{b}\right)\times\int_0^t\left|\tilde{\vartheta}(t)\right|^{\left(\frac{a}{b}-1\right)}dt\,\mathrm{sign}\left(\tilde{\vartheta}(t)\right)\right)\}$$

Using dynamic model and simplifications yields:

$$\dot{V}_{\text{APISMC}}\left(s_{\vartheta},\tilde{\mathcal{Q}}\right)=\tilde{\mathcal{Q}}^{\mathrm{T}}\mathrm{L}\,\dot{\tilde{\mathcal{Q}}}+\sum s_{\vartheta}^{T}$$
$$+\sum s_{\vartheta}\left(-\delta_{\vartheta}-\left(\hat{\gamma}_0+\hat{\gamma}_1\vartheta+\hat{\gamma}_2\vartheta^2\right)\text{sign}\left(s_{\vartheta}\right)\right) \tag{36}$$

Consequently,

$$\dot{V}_{\text{APISMC}}\left(s_{\vartheta},\tilde{\mathcal{Q}}\right)\le\tilde{\mathcal{Q}}^{\mathrm{T}}\mathrm{L}\,\dot{\tilde{\mathcal{Q}}}-\sum\{\delta_{\vartheta}s_{\vartheta}+\left(\hat{\gamma}_0+\hat{\gamma}_1\vartheta+\hat{\gamma}_2\vartheta^2\right)s_{\vartheta}\} \tag{37}$$

Using (35) and (36), yields

$$\dot{V}_{\text{APISMC}}\left(s_{\vartheta},\tilde{\mathcal{Q}}\right)\le$$
$$\sum\tilde{\gamma}_0\left(\frac{\dot{\hat{\gamma}}_0}{\beta_0}-s_{\vartheta}\right)+\tilde{\gamma}_1\left(\frac{\dot{\hat{\gamma}}_1}{\beta_1}-s_{\vartheta}\vartheta\right)+\tilde{\gamma}_2\left(\frac{\dot{\hat{\gamma}}_2}{\beta_2}-s_{\vartheta}\vartheta^2\right)-\sum\delta_{\vartheta}s_{\vartheta} \tag{38}$$

Applying adaptive laws (31) and simplifications yields

$$\dot{V}_{\text{APISMC}}\left(s_{\vartheta},\tilde{\mathcal{Q}}\right)\le-\sum\delta_{\vartheta}s_{\vartheta} \tag{39}$$

Henceforth, it is duly acknowledged that the achieved state of the control algorithm stability has been successfully materialized.

8. Obtained results

We will now proceed to showcase the results that have been achieved in various scenarios in the subsequent section to confirm the effectiveness of the ATSMC scheme proposed in this study. An external disturbance of significant magnitude (as defined in Eq. 40) has been introduced into the system's dynamic Eq.s to assess the robustness of the controller. The specific model parameters of the Autonomous Underwater Vehicle (AUV) can be found in reference [25].

The selected simulation environment for this endeavor is the renowned MATLAB/Simulink platform. Its immense capability to efficiently simulate linear, nonlinear, multi-rate, variable-step,

and fixed-step systems, coupled with its vast collection of toolboxes dedicated to swift research and development tasks, render it the prime choice for this specific undertaking.

$$d = 3\begin{bmatrix} \sin\left(\frac{t}{15}\right)\cos\left(\frac{t}{5}\right) \\ 0 \\ \sin\left(\frac{t}{15}\right)\sin\left(\frac{t}{5}\right) \\ \cos\left(\frac{t}{15}\right) \end{bmatrix}^{T} \left(u_s\left(t-35\right)-u_s\left(t-55\right)\right) \tag{40}$$

In the initial situation, the robot effectively followed the intended trajectory, commencing from any random location within the Cartesian space. (Refer to Fig. 3 for visual representation)

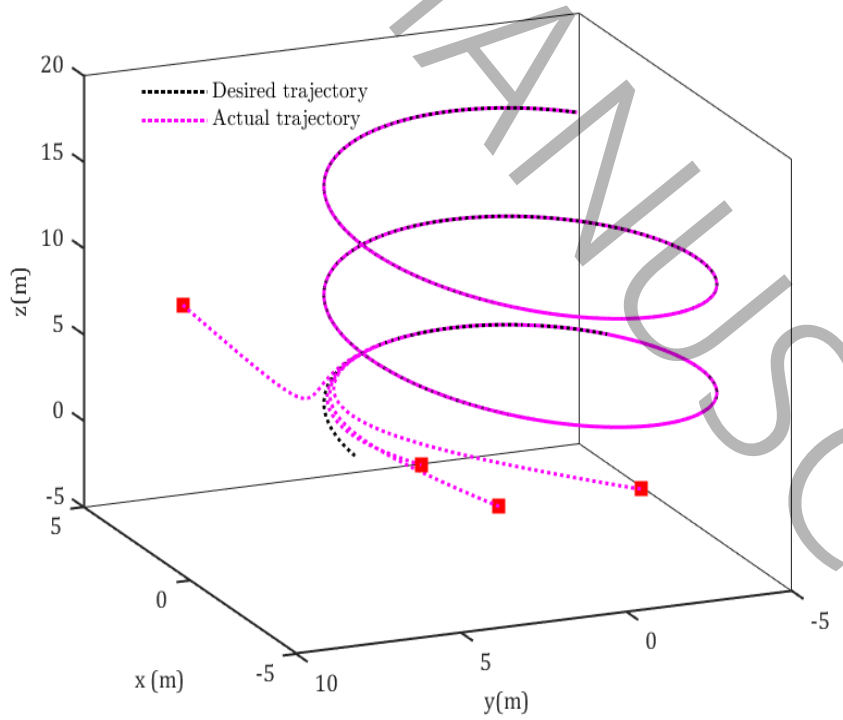

Fig3. The reference and the real motion path (starting from four deferent points) for the AUV in 3D space.

In an alternative scenario for evaluating the effectiveness of the proposed method, thorough comparisons were made between the feedback linear (FL), sliding mode control (SMC), the methodology outlined in reference [10], and Adaptive nonsingular fast integral-type terminal sliding mode control techniques. The movement trajectory of the robot and the reference trajectory in both 3D and 2D spaces, amidst external disturbances, were depicted in Fig. 4-5 for all controllers under scrutiny.

Between 30 to 50 seconds into the simulation, a significant external disturbance was introduced into the system. Noteworthy is that the controllers demonstrated their resilience by promptly addressing the situation. Subsequently, the results pertaining to position tracking error and the 3-axis control inputs were illustrated in Fig. 6-7.

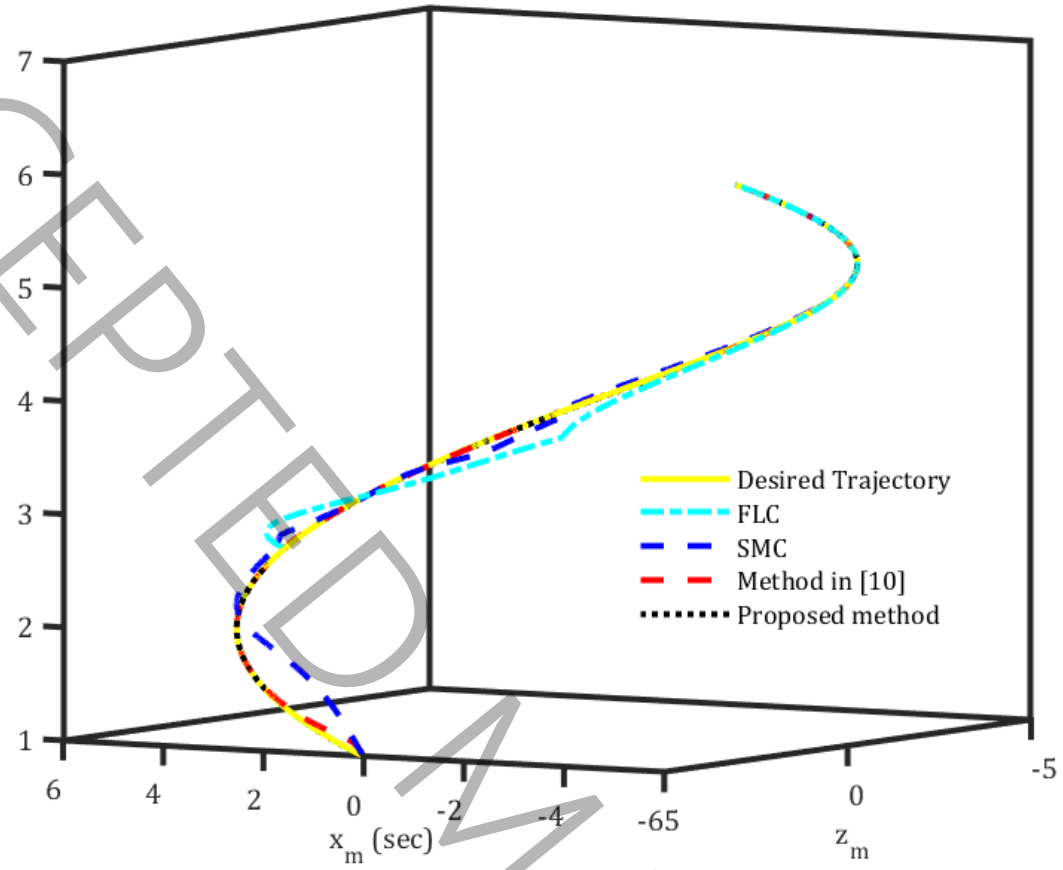

Fig 4. Comparison of various algorithms for a 3D motion path

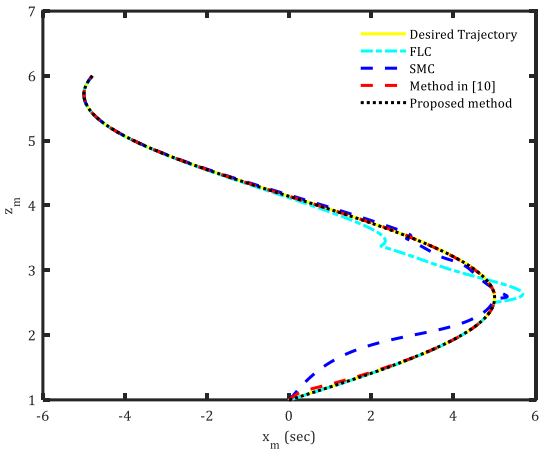

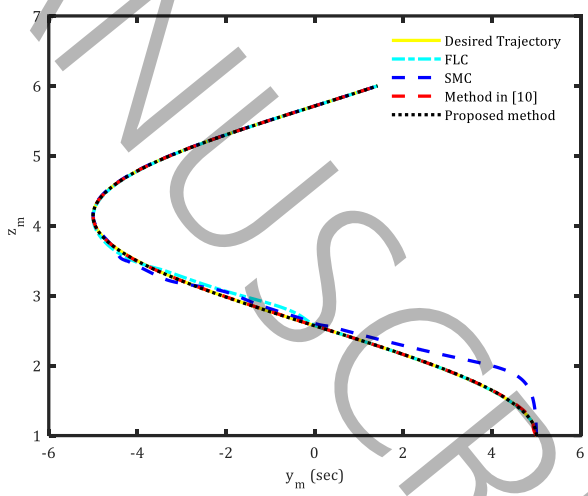

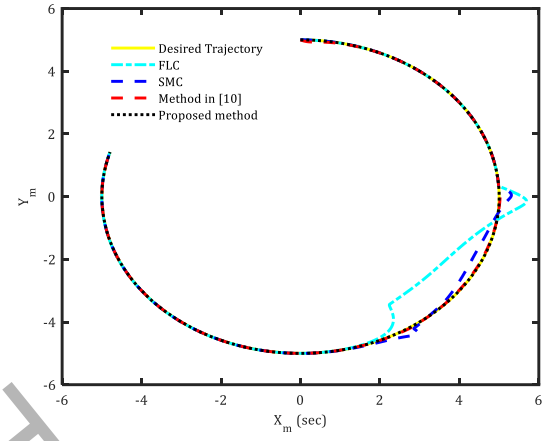

Fig 5. Comparison of various algorithms for a 2D motion path

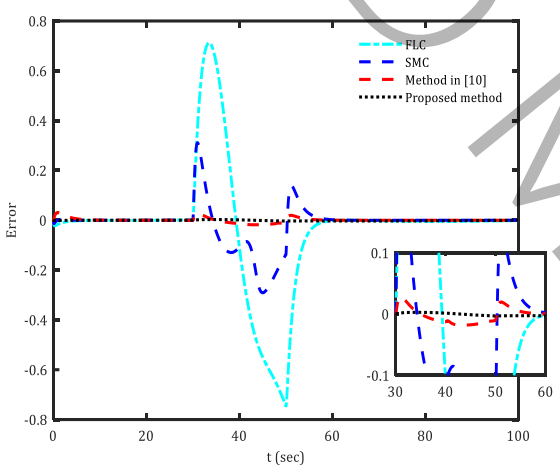

a) x-direction

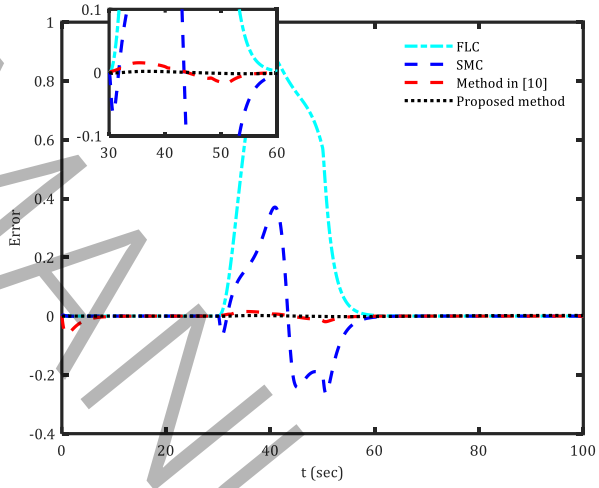

b) y-direction

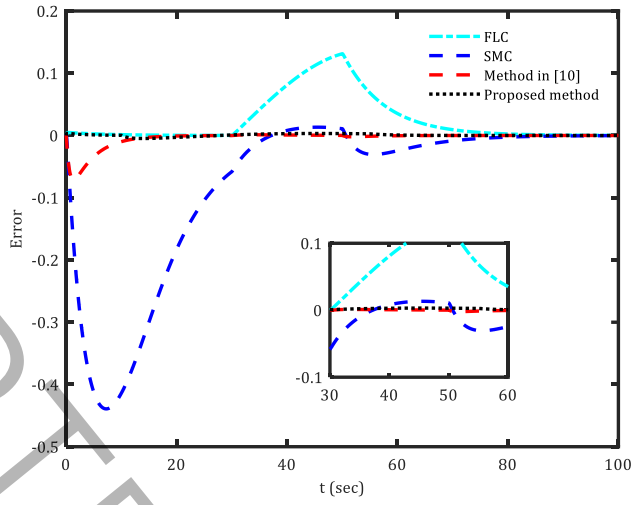

c) z-direction

Fig 6. Tracking errors in the x/y/z-direction for all compared controllers

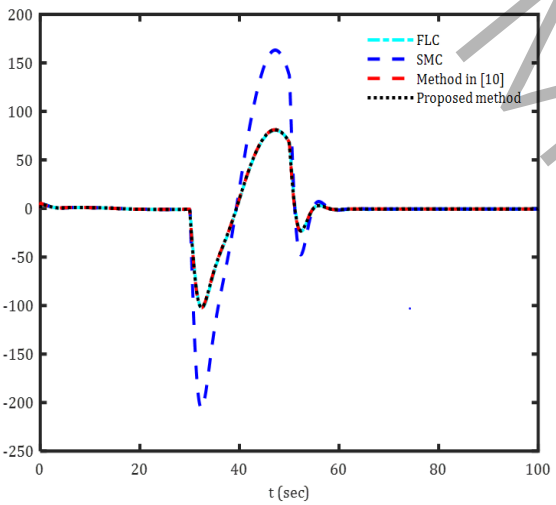

a) Control input (N) in x-direction

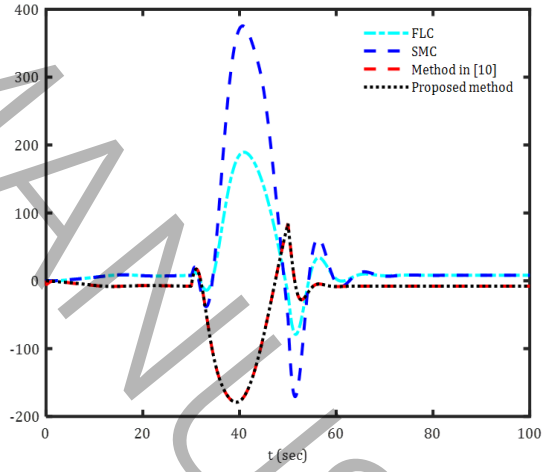

b) Control input (N) in y-direction

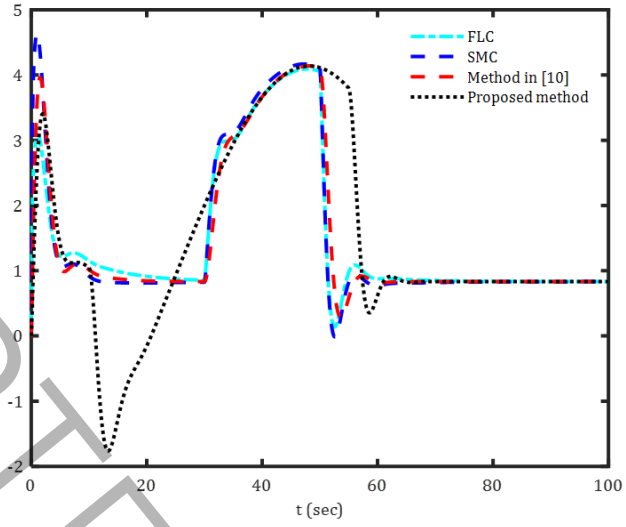

c) Control input (N) in z-direction

Fig 7. Control input (N) for all compared controllers

In summation, the adaptive robust nonlinear control strategy outlined in this document demonstrates a high level of competency in effectively tracing trajectories, even when faced with uncertainties and disturbances. While the efficiency of all algorithms discussed in this article is deemed acceptable.

5 Conclusions

A highly advanced tracking controller utilizing an inner/outer-loop approach has been developed to address the trajectory tracking challenges of the AUVs in the presence of ocean current disturbances. In comparison to traditional sliding mode controllers, the incorporation of an adaptive integral sliding mode surface significantly boosts the robustness of the control system, while the double loop controller structure greatly improves its dynamic performance. Notably, the new switching method successfully mitigates the sliding mode chattering of the AUVs. The

asymptotic convergence of tracking error in joint space is proven using the Lyapunov direct method. Furthermore, this innovative approach simplifies the algorithm, and streamlines implementation on the AUVs embedded platform. The outcomes demonstrate that the tracking controller for the AUVs functions effectively with both stability and robustness.

References

[1] F. S. Tabataba'i-Nasab, A. Keymasi Khalaji, S. A. A. Moosavian, Adaptive nonlinear control of an autonomous underwater vehicle. Transactions of the Institute of Measurement and Control, 41(11) (2019) 3121-31.

[2] F. S. Tabatabaee-Nasab, S. A. A. Moosavian, A. K. Khalaji, Adaptive fault-tolerant control for an autonomous underwater vehicle, Robotica, 40(11), (2022) 4076-89.

[3] F. S. Tabatabaee-Nasab, S. A. A. Moosavian, Uncertain Object Manipulation Using Adaptive Multiple Impedance Control, In2023 11th RSI International Conference on Robotics and Mechatronics (ICRoM) (2023) 408-413.

[4] S. Khankalantary, M. Hajizadeh, K. Heidari, H. Mohammadkhani, Impact Time Guidance Law against Maneuvering Targets Using Sliding Mode Control. Amirkabir Journal of Mechanical Engineering, 53(2) (2021) 913-22.

[5] A. H. Abolmasoumi, M. Soleymani, A. Shahmohammadi, M. Mehdizadeh, Design and Implementation of Fast Terminal Sliding Mode Control for Vehicle Lane Keeping by Using Virtual Prototyping Simulations, Amirkabir Journal of Mechanical Engineering, 49(2) (2017) 371-8.

[6] M. Kim, H. Joe, J. Kim, S. C. Yu, Integral sliding mode controller for precise manoeuvring of autonomous underwater vehicle in the presence of unknown environmental disturbances, International Journal of Control, 88(10) (2015) 2055-65.

[7] E. Zakeri, S. Farahat, S. A. Moezi, A. Zare, Robust sliding mode control of a mini unmanned underwater vehicle equipped with a new arrangement of water jet propulsions: Simulation and experimental study, Applied Ocean Research, 59 (2016) 521-42.

[8] F. S. Tabataba'i-Nasab, S. A. A. Moosavian, A. K. Khalaji, Tracking Control of an Autonomous Underwater Vehicle: Higher-Order Sliding Mode Control Approach, In2019 7th International Conference on Robotics and Mechatronics (ICRoM) (2019) 114-119.

[9] S. An, L. Wang, Y. He, J. Yuan, Adaptive backstepping sliding mode tracking control for autonomous underwater vehicles with input quantization, Advanced Theory and Simulations, 5(4) (2022) 2100445.

[10] T. Elmokadem, M. Zribi, and K. Youcef-Toumi, Terminal sliding mode control for the trajectory tracking of underactuated Autonomous Underwater Vehicles, Ocean Engineering, 129 (2017) 613-625.

[11] J. H. Kim, S. J. Yoo, Distributed event-driven adaptive three-dimensional formation tracking of networked autonomous underwater vehicles with unknown nonlinearities, Ocean engineering, 233 (2021) 109069.

[12] H. Esfandiar, S. Daneshmand, Kermani, On the control of a single flexible arm robot via Youla-Kucera parameterization, Robotica, 34(1) (2016) 150-72.

[13] H. Esfandiar, S. Daneshmand, Closed loop control of the planar flexible manipulator via Youla-Kucera parameterization, Journal of Mechanical Science and Technology, 27 (2013) 3243-52.

[14] M. Ghafouri, S. Daneshmand, Design and evaluation of an optimal fuzzy pid controller for an active vehicle suspension system, Transactions of FAMENA, 41(2) (2017) 29-44.

[15] J. J. Slotine, and W. Li, Applied nonlinear control. Upper Saddle River, NJ: Prentice Hall, 1991.

[16] Y. Pan, W. Wei, K. Furuta, Hybrid sliding sector control for a wheeled mobile robot. Proceedings of the Institution of Mechanical Engineers, Part I: Journal of Systems and Control Engineering, 222(8) (2008) 829-37.

[17] T. I. Fossen, S. I. Sagatun. Adaptive control of nonlinear underwater robotic systems, (1991) 95-105.

[18] R. Cristi, F. A. Papoulias, A. J. Healey, Adaptive sliding mode control of autonomous underwater vehicles in the dive plane. IEEE journal of Oceanic Engineering, 15(3) (1990) 152-60.

[19] D. R. Yoerger, J. J. Slotine, Adaptive sliding control of an experimental underwater vehicle. InProceedings. 1991 IEEE International Conference on Robotics and Automation (1991) 2746-2751.

[20] M. L. Corradini, G. A. Orlando, discrete adaptive variable-structure controller for MIMO systems, and its application to an underwater ROV, IEEE Transactions on Control Systems Technology, 5(3) (1997) 349-59.

[21] L. Qiao, W. Zhang, Double-loop chattering-free adaptive integral sliding mode control for underwater vehicles, InOCEANS 2016-Shanghai, (2016) 1-6.

[22] L. Qiao, W. Zhang, Adaptive second-order fast nonsingular terminal sliding mode tracking control for fully actuated autonomous underwater vehicles, IEEE Journal of Oceanic Engineering, 44(2) (2018) 363-85.

[23] N. Maghooli, F. S. Tabatabaee-Nasab, S. A. A. Moosavian, Self-Tuning Robust Tracking Control for Autonomous Underwater Vehicles. In2022 10th RSI International Conference on Robotics and Mechatronic, (2022) 279-284.

[24] T. T. J. Prestero, Verification of a six-degree of freedom simulation model for the REMUS autonomous underwater vehicle, PhD diss., Massachusetts institute of technology, 2001.